DEVELOPMENT OF AN ENGINEERING MODEL OF THE AMPLITUDE AND DURATION EFFECTS OF BASIN GENERATED SURFACE WAVES

Paul G. Somerville, Nancy Collins, Robert Graves, and Arben Pitarka

URS Group, Inc., Pasadena, CA

Abstract

Basin waves are polarized predominantly in the directions parallel to and normal to the edge of the basin, consistent with the assumption made by Joyner (2000). There are significant differences between the amplitudes of the horizontal component parallel to the basin edge, which is predominantly Love waves, and the horizontal component perpendicular to the basin edge, which is predominantly Rayleigh waves, although these amplitudes will be affected by the relative strength of the incoming waves, which depends on focal mechanism and other factors. This is also consistent with the assumption made by Joyner (2000). There is a significant dependence of the ground motion amplitude and duration on basin depth. Basin depth dependence was not included in the Joyner (2000) model. When depth increases away from the basin edge (i.e. when basin depth and basin edge distance are correlated), this can cause ground motion amplitudes and durations to increase away from the basin edge. The Husid plot derived from the velocity waveform provides an appropriate duration measure that is independent of the absolute amplitude level.

Introduction

Joyner (2000) developed a procedure for modifying standard spectral attenuation relations to account for the amplitude effects of surface waves in deep sedimentary basins. The objective of this project is to extend his work so that it is more broadly applicable in earthquake engineering. We are extending the model to include duration in addition to spectral amplitudes. We are extending the model to include basins other than the Los Angeles basin. In particular, we are including data from shallower basins, such as the San Bernardino, San Fernando, Santa Clara, and Eel River basins, in which the basin effects are expected to extend to shorter periods. We are extending the lower bound of the period range covered by Joyner from 3 seconds to 1 second, which will make the model relevant to a much larger number of structures. The result of this study will be a model, suitable for earthquake engineering application, that modifies standard ground motion models to account for the amplitude and duration effects of basin generated surface waves. This paper describes results that have been obtained to date.

Mode of Generation of Basin Waves

The mode of generation of basin-trapped waves is illustrated schematically in Figure 1. If a seismic wave enters a basin through its edge, it can become trapped within the basin if post-critical incidence angles develop. The resulting total internal reflection at the base of the layer is

illustrated at the top right of Figure 1. In the lower part of Figure 1, simple calculations of the basin response are compared with those for the simple horizontal layered model shown on the left side of the figure. In each case, a plane wave is incident at an inclined angle from below. The left side of the figure shows the amplification due to impedance contrast effects that occurs on a flat soil layer overlying rock (bottom) relative to the rock response (top). A similar amplification effect is shown for the basin case on the right side of the figure. However, in addition to this amplification, the body wave entering the edge of the basin becomes trapped, generating a surface wave that propagates across the basin. Current empirical ground motion attenuation relations do not distinguish between sites located inside and outside basins, and tend to underestimate the ground motions recorded in basins.

Joyner Model of Basin Effects

The basic concept underlying the Joyner (2000) model is that ground motions from an earthquake occurring outside a basin attenuate normally until they reach the basin edge, and then attenuate at a slower rate after entering the basin. The ground motion model is given by the equation:

$$\text{Log } y = f(M, R_E) + c + b\,R_B$$

In this equation, y is the response spectral amplitude, $f(M, R_E)$ is an attenuation relation for non-basin conditions, M is moment magnitude, R_E is the distance from the earthquake to the basin edge, and R_B is the distance from the basin edge to the recording site. The parameter c is a measure of the coupling between the incident body waves and the surface waves in the basin, and the parameter b controls the attenuation with distance in the basin. Parameters b and c are period dependent parameters that are derived from the data. We are extending this model to include the effect of the depth H to crystalline bedrock below the recording site:

$$\text{Log } y = f(M, R_E) + c + b\,R_B + a\,H$$

The Joyner model was developed for three components: parallel to the basin edge, perpendicular to the basin edge, and vertical. The perpendicular attenuation is found to be lower than the parallel attenuation. Joyner attributes this to the lower attenuation of Rayleigh waves (on the perpendicular component) than Love waves (on the parallel component) due to differences in the Q (damping) of P and S waves. However, unless the ray path is normal to the basin edge, this simple partitioning of wave types does not hold, because the site-to-source azimuth and the strike of the basin edge are independent variables. The Rayleigh waves should be on the radial component and the Love waves should be on the transverse component. For earthquakes located north of the Los Angeles basin, Joyner's assumption is reasonably valid, but for the Landers, Big Bear and Hector Mine earthquakes, the Love waves are closer to being perpendicular to the basin edge than parallel. However, it is possible that lateral refraction of the surface waves at the edge of the basin may tend to orient the waves in the directions assumed by Joyner.

Analysis of Polarization of Basin Waves

In Joyner's model, differences are recognized between the basin edge parallel and basin edge normal components. This model is based on the expectation that there is lateral refraction of surface waves at the basin edge. Alternative models could be based on the radial and tangential components, or the average horizontal component. Our first goal is to determine whether the data are consistent with Joyner's assumption.

We illustrate our analysis using the recordings of the 1999 Hector Mine earthquake in the San Bernardino basin. Figure 2 is a map showing the three fault segments of the Hector Mine earthquake and the locations of strong motion recording stations. The small shaded box contains stations located in and near the San Bernardino basin, shown in more detail in Figures 3 and 4. Profile A-A' in Figures 3 and 4 crosses the San Bernardino basin at right angles to the San Andreas fault, which forms the northeastern boundary of the basin. The San Jacinto fault forms the southwestern boundary of the basin. The basin structure is shown by the depth contours to bedrock (in km) and by the cross sections in Figure 4. The basin gradually thickens away from the San Andreas fault, and reaches a maximum depth of about 1 km near the San Jacinto fault, which is associated with a marked step in basement topography.

The lowpass filtered velocity waveforms of the Hector Mine earthquake recorded in and near the San Bernardino basin along profile A-A' are shown in Figure 5. At the top of Figure 5, we show the tangential (N154E) component on the left and the radial (N244E) component on the right. Because of the orientation and strike-slip mechanism of the Hector Mine earthquake, the radial direction is nodal, and nearly all of the energy is on the orthogonal tangential component. This can be seen in the waveforms of the closest recording station 5331 at the top of Figure 5, which lies just north of the San Andreas fault, outside the basin. There are large SH and Love waves on the N154E tangential component because they are near the maximum in the radiation pattern, and small Rayleigh waves on the radial N244E component because they are almost nodal.

At the bottom of Figure 5, we show the basin edge parallel (N310) component on the left and the basin edge normal (N220E) component on the right. Comparing these profiles with those at the top of Figure 5, we can see a clear change in the polarization of the ground motion. At basin stations (distances between 7 and 12 km from the San Andreas fault), the large SH and Love waves are much better separated from the nodal Rayleigh waves in the basin edge orientation shown at the bottom of Figure 5 than in the radial and tangential orientation shown at the top of Figure 5. In contrast, for station 5331 described above, the separation between these wave types for the basin orientation is degraded as expected, because this station is outside the basin.

Additional support for this interpretation of the polarization of the ground motions in the basin edge normal and basin edge parallel directions comes from polarization analysis using the method of Vidale (1986). Figure 6 shows the results of this analysis for the recording of the Hector Mine earthquake at station sbmv, located within the basin. The analysis on the left side of the figure is for the radial and tangential directions, and the analysis on the right side of the figure is for the basin edge normal and basin edge parallel directions. The latter orientation gives

strike angles closer to 90 degrees, representing Love waves with particle motion parallel to the basin edge.

The data analyses shown in Figures 5 and 6 provide clear evidence of lateral refraction of surface waves at the basin edge. We conclude that basin waves are polarized predominantly in the directions parallel to and normal to the edge of the basin. This is consistent with the assumption made by Joyner (2000).

Generally, lateral refraction will cause SH and Love waves to be preferentially oriented on the basin edge parallel component, and Rayleigh waves to be oriented on the basin edge normal component, as illustrated in the Hector Mine recordings shown in Figures 5 and 6. Consequently, we expect these two components to have different amplitudes and to attenuate differently with distance away from the basin edge. For the Hector Mine recordings, radiation pattern effects caused a large difference in amplitude between these two components. These observations justify the use of separate attenuation functions for the basin edge normal and basin edge parallel components in the Joyner (2000) model. In that model, the basin edge parallel component attenuates more rapidly than the basin edge normal component.

Arias Intensity and Duration of Basin Waves

Since our basin ground motion model will include both amplitude and duration parameters, we plan to use a definition of duration that does not depend on the absolute level of the ground motion. We have evaluated the effectiveness of the Husid duration (Husid, 1969) of the velocity time history, which is used in the Abrahamson and Silva (1997b) model, as a measure of the duration of surface waves.

The method that we use to measure the Arias intensity and duration of basin waves is illustrated in Figure 7. This figure shows the recorded velocity time histories of the radial, tangential, radial, basin edge parallel, basin edge normal components, and the cumulative square of each time history (Husid, 1969), which represents the energy. The Arias intensity is defined as the total value of the cumulative energy, and the duration is measured over the time interval in which the energy grows from 5% to 90% of its total value.

Effect of Basin Depth and Distance from Basin Edge on Basin Wave Amplitudes and Durations

We have used the strong motion recordings of the 1999 Hector Mine earthquake recorded in the San Bernardino Basin to analyze the effect of basin depth and distance from basin edge on basin wave amplitudes and durations. As shown in Figure 8, the peak velocity increases markedly when the waves enter the San Bernardino basin, and grows in amplitude with increasing distance from the basin edge, even though the distance from the source is increasing. This is due to the trapping of body waves that enter the basin, generating surface waves. Once the waves have crossed the basin and left the basin, their amplitudes begin to decay again. A clear correlation of peak velocity with basin depth is shown in Figure 9. When depth increases away from the basin edge (i.e. when basin depth and basin edge distance are correlated), this can cause ground motion amplitudes to increase away from the basin edge.

The Arias intensity data (Figures 10 and 11) show trends that are generally similar to those for peak velocity that have just been described. The amplification in Arias intensity that is caused by the basin is significantly larger than for peak velocity. This reflects the increase in duration as well as in the amplitude of the waves that become trapped in the basin. The Arias intensity also has a stronger dependence on basin depth, with values increasing as the trapped waves propagate away from the source across the basin.

The duration of ground motion (Figures 12 and 13) also shows trends that are generally similar to those for peak velocity. The duration increases when the waves enter the basin, and decreases again upon leaving the basin but remains larger than the duration of the waves that entered the basin. Unlike peak ground motion, which tends to decrease with increasing distance from the earthquake, duration tends to increase with distance. The duration measurements on the basin edge parallel component have much more stable behavior than those of the basin edge normal component. This reflects the fact that the basin edge parallel waves, consisting of mainly of Love waves, have much larger amplitudes than the basin edge normal waves, which consist mainly of Rayleigh waves, due to the mechanism of the Hector Mine earthquake.

Development of Engineering Model of Basin Wave Amplitudes and Durations

Joyner (2000) developed a procedure for modifying standard spectral attenuation relations to account for the amplitude effects of surface waves in deep sedimentary basins. The objective of this project is to extend his work so that it is more broadly applicable in earthquake engineering. We are extending the model to include duration in addition to spectral amplitudes. We are extending the model to include basins other than the Los Angeles basin. In particular, we are including data from shallower basins, such as the San Bernardino, San Fernando, Santa Clara, and Eel River basins, in which the basin effects are expected to extend to shorter periods. We are extending the lower bound of the period range covered by Joyner from 3 seconds to 1 second, which will make the model relevant to a much larger number of structures. The result of this study will be a model, suitable for earthquake engineering application, that modifies standard ground motion models to account for the amplitude and duration effects of basin generated surface waves.

Conclusions

Polarization of Surface Waves

Basin waves are polarized predominantly in the directions parallel to and normal to the edge of the basin, with Love waves predominating on the parallel direction and Rayleigh waves predominating on the normal direction. This is consistent with the assumption made by Joyner (2000) and is caused by the lateral refraction of surface waves at the basin edge.

Differences between Basin Edge Parallel and Normal Components

There are significant differences between the amplitudes of the horizontal component parallel to the basin edge, which is predominantly Love waves, and the horizontal component perpendicular to the basin edge, which is predominantly Rayleigh waves, although these amplitudes will be affected by the relative strength of the incoming waves, which depends on

focal mechanism and other factors. This is consistent with the assumption made by Joyner (2000).

Dependence of Amplitude on Basin Depth

There is a significant dependence of the ground motion amplitude on basin depth. When depth increases away from the basin edge (i.e. when basin depth and basin edge distance are correlated), this can cause ground motion amplitudes to increase away from the basin edge.

Duration measure

The Husid plot derived from the velocity waveform provides an appropriate duration measure that is independent of the absolute amplitude level.

Dependence of Duration on Basin Depth

There is a significant dependence of the ground motion duration on basin depth. When depth increases away from the basin edge (i.e. when basin depth and basin edge distance are correlated), this can enhance the tendency of ground motion duration to increase away from the basin edge.

References

Abrahamson, N.A. and W.J. Silva (1997b). Empirical duration relations for shallow crustal earthquakes. Written communication.

Husid, R.L. (1969). Analisis de terremotos: Analisis General, Revista del IDIEM, 8, 21-42, Santiago, Chile.

Joyner, W.B. (2000). Strong motion from surface waves in deep sedimentary basins. *Bull. Seism. Soc. Am*., 90, S95-S112.

Vidale, J.E. (1986). Complex polarization analysis of particle motion. Bull. Seism. Soc. Am., 76, 1393-1405.
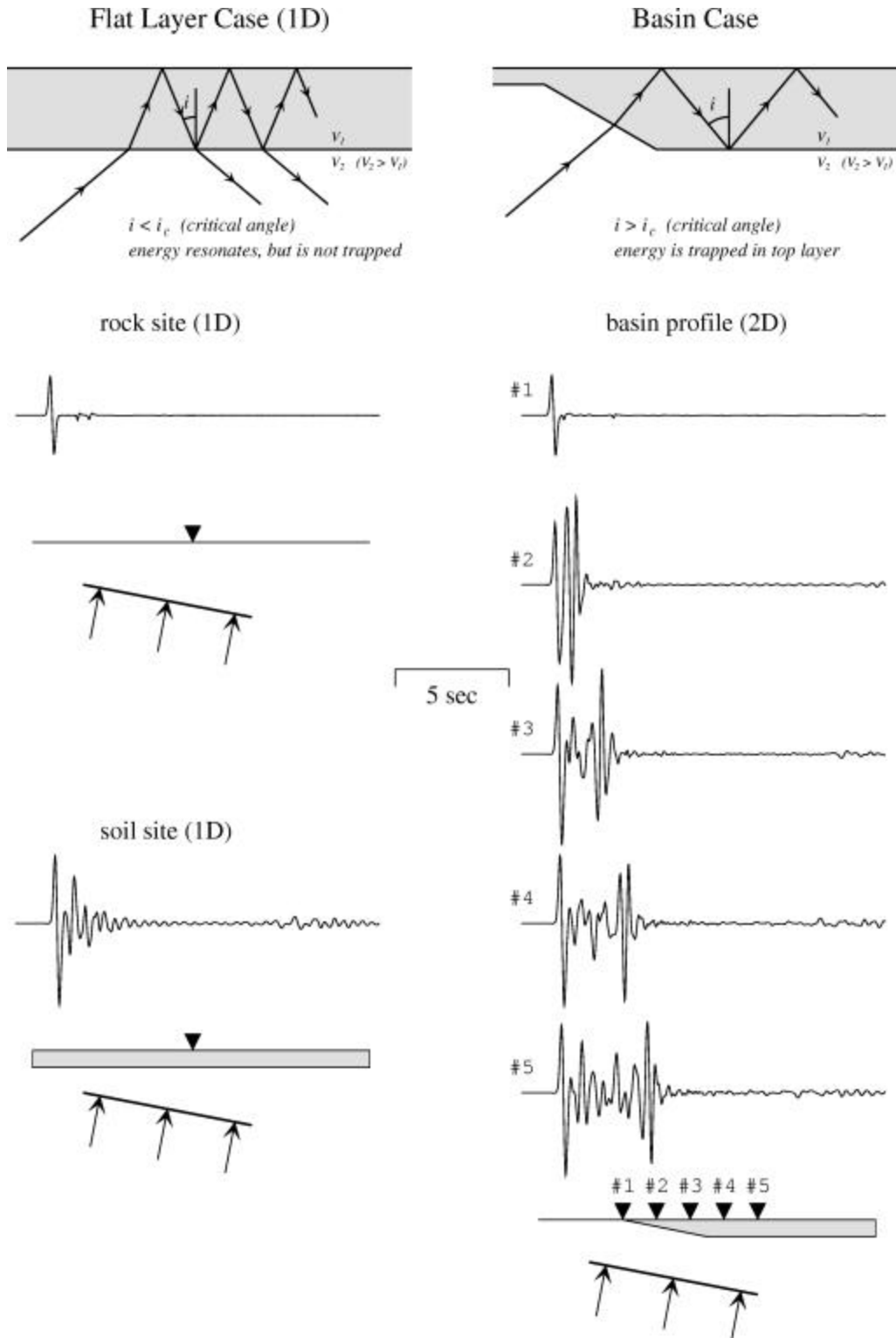
Figure 1. Schematic diagram showing that seismic waves entering a sedimentary layer from below can escape if the layer is flat (left), but can become trapped in the layer if it has varying thickness, for example when waves enter a basin through its edge (right). Source: Graves, 1993.
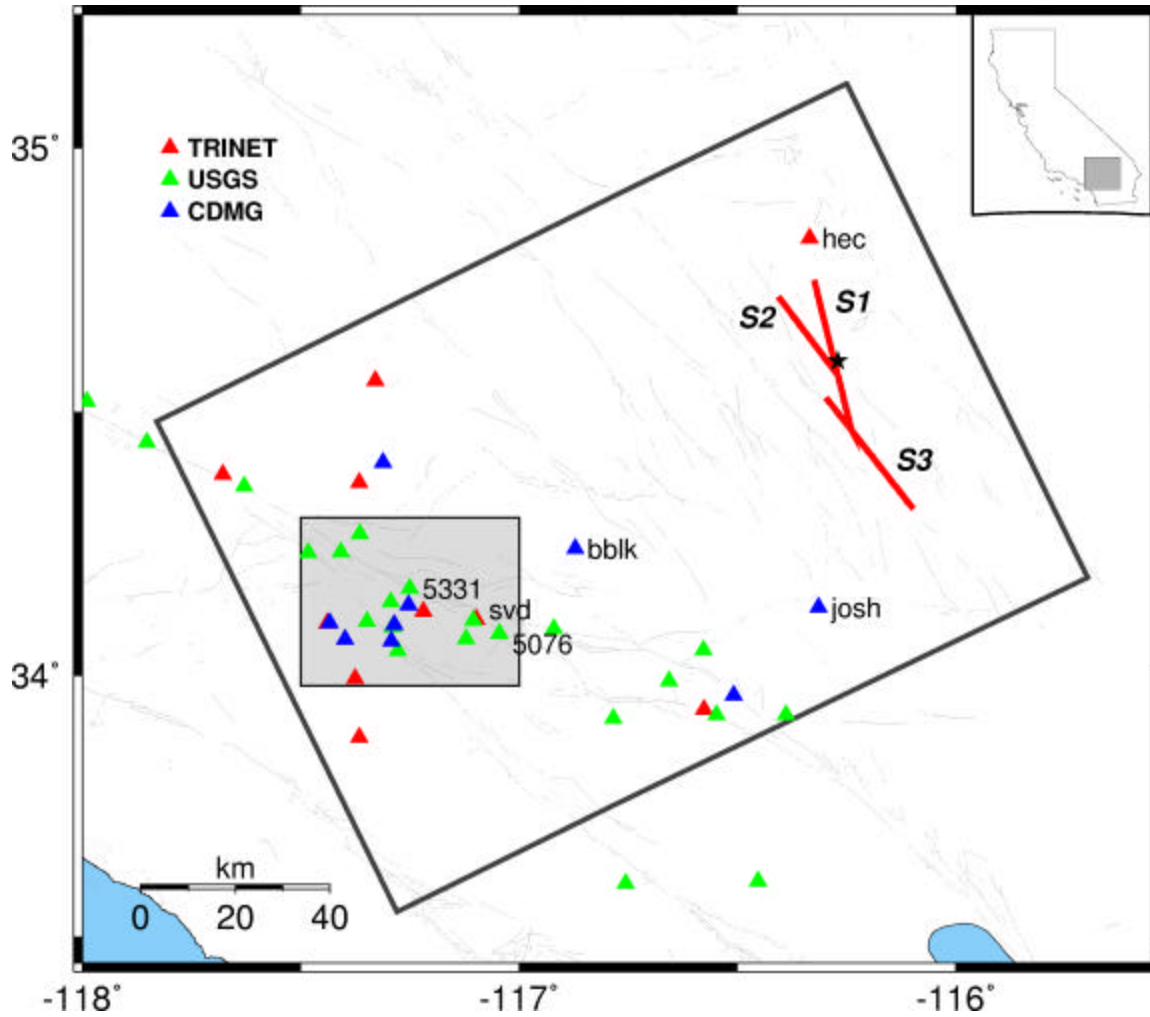
Figure 2. Map showing location fault segments S1, S2 and S3 of the 1999 Hector Mine earthquake, and strong motion recording stations including those in the San Bernardino Basin (small box).
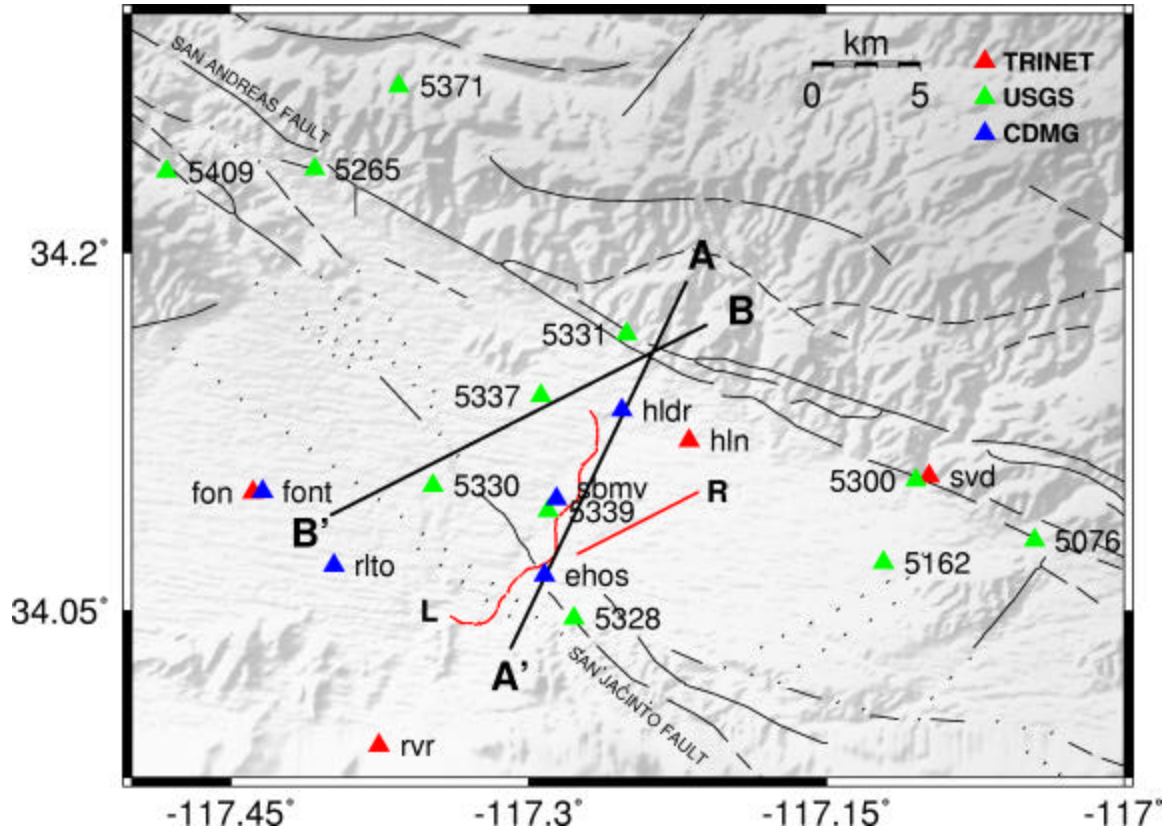
Figure 3. Locations of the San Andreas and San Jacinto faults, and strong motion recording stations in the San Bernardino Basin (small box in Figure 2).
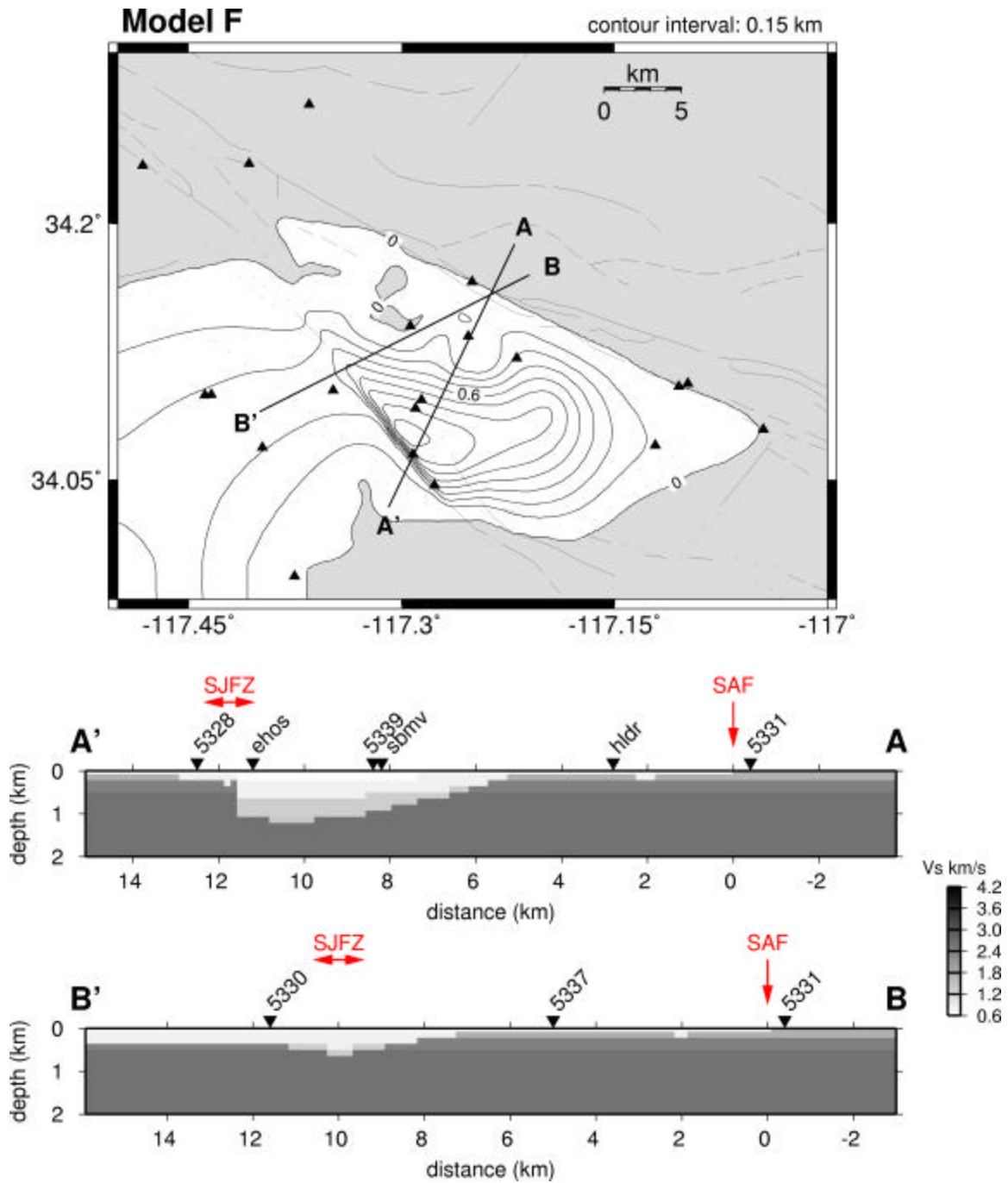
Figure 4. Map of the San Bernardino basin showing contours in depth to bedrock (top) and seismic velocity profiles along cross sections A-A' and B-B' (bottom).

Figure 5. Top: Profiles of ground velocity of the 1999 Hector Mine earthquake recorded across profile A-A' in Figures 3 and 4 for the tangential (154) component (left) and the radial (244) component (right). Bottom: Profiles of ground velocity of the 1999 Hector Mine earthquake recorded across profile A-A' in Figures 3 and 4 for the basin edge parallel (130) component (left) and the basin edge normal (220) component (right).
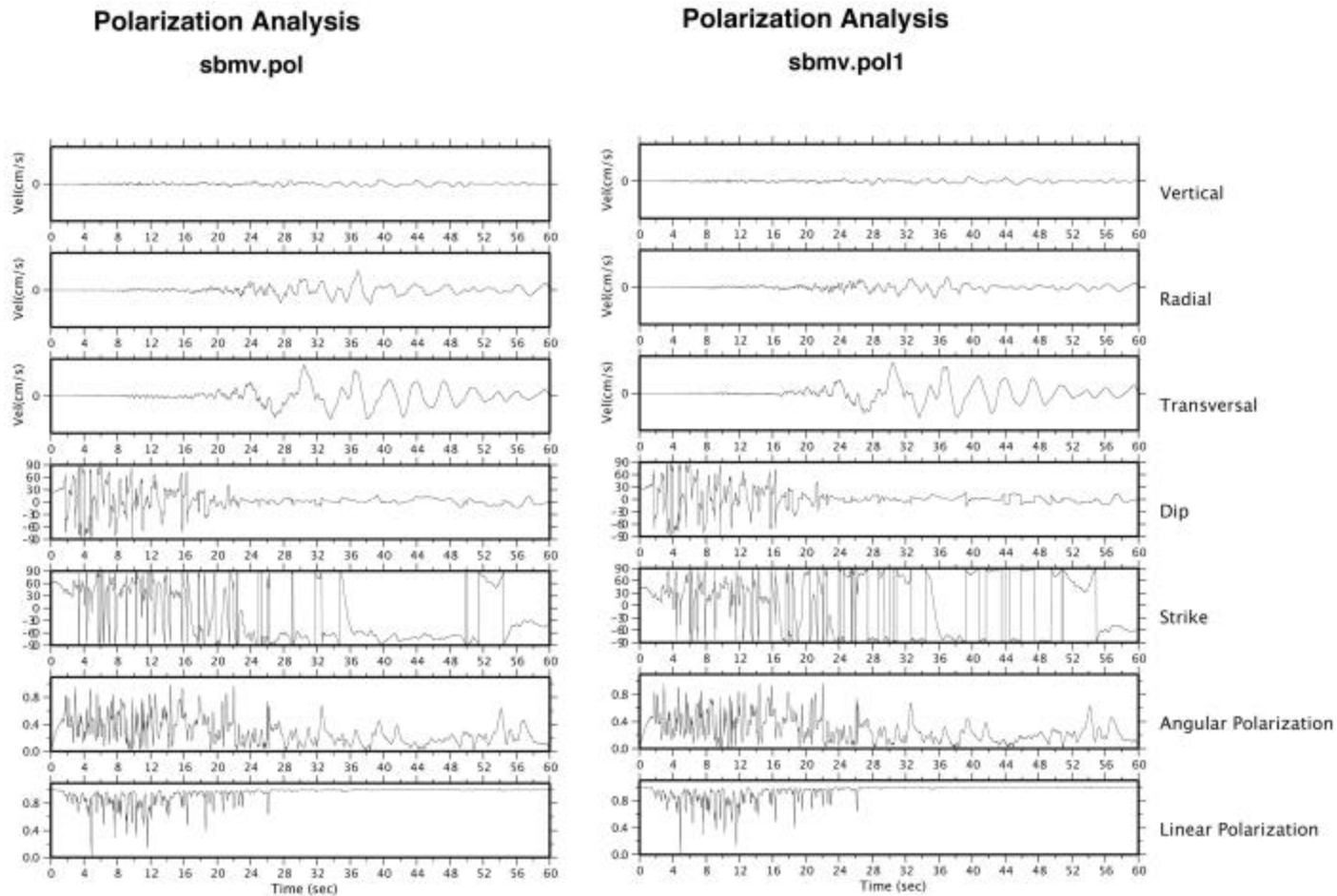
Figure 6. Polarization analysis of the Mountain View recording of the 1999 Hector Mine earthquake. The top three traces on the left are the vertical, radial and transverse components of velocity. The top three traces on the right are the vertical, basin edge normal, and basin edge parallel components of velocity. The bottom four traces on each side are the strike and dip of the maximum polarization, the angular polarization, and linear polarization of the motion, as defined by Vidale (1986). The strike for the basin edge normal and basin edge parallel components (right) is very close to +/- 90 degrees, but is about +/- 60 degrees for the radial and tangential components (left). This indicates that the ground motions are polarized in the basin edge normal and basin edge parallel directions.

Hector Mine - Velocity Duration (0.05-0.90)
San Bernardino - Mtn. View & Cluster (sbmv)
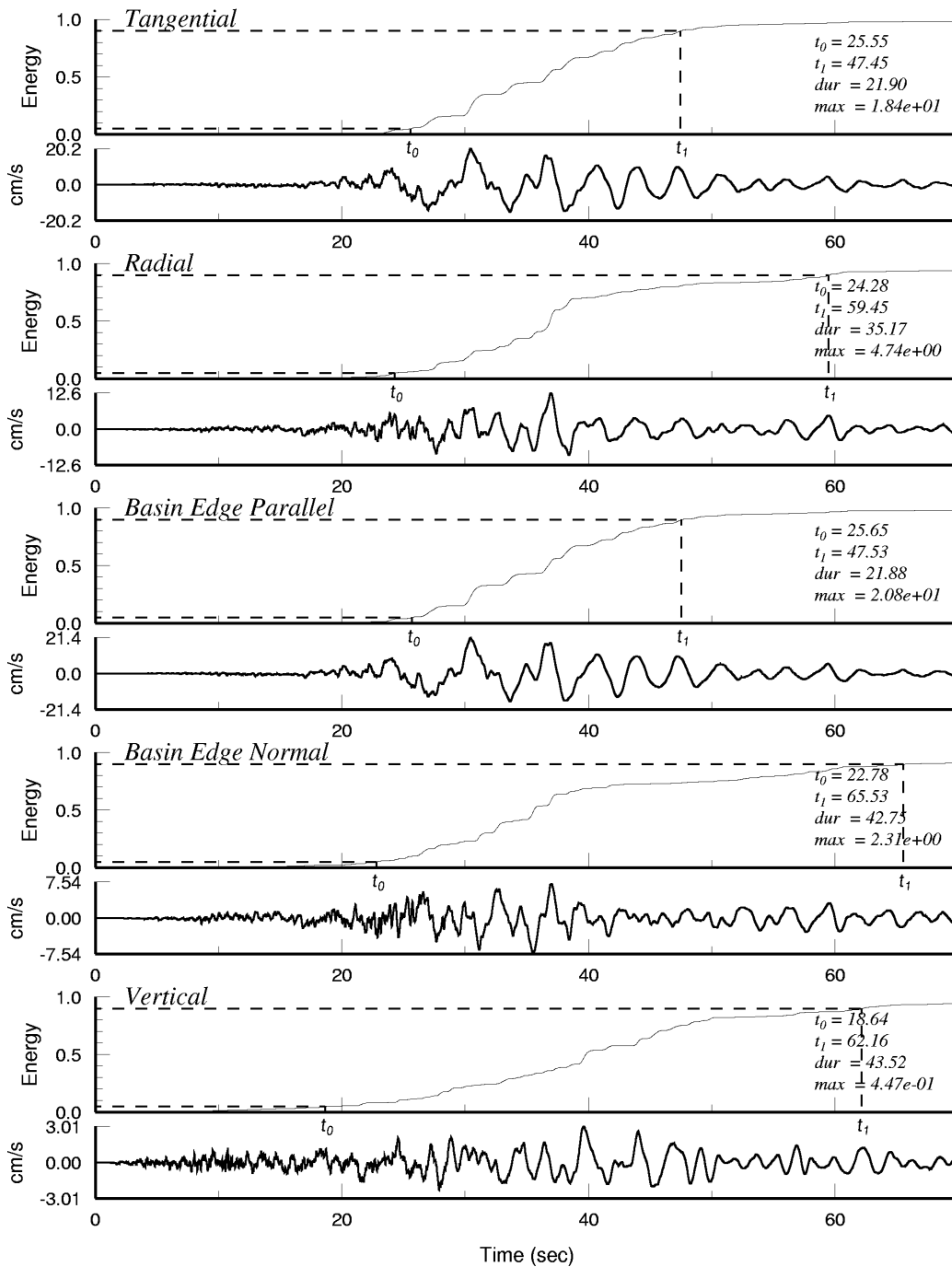
Figure 7. Husid plots of the Mountain View recording of the 1999 Hector Mine earthquake earthquake for five components of ground motion: tangential, radial, basin edge parallel, basin edge normal, and vertical. For each pair of traces, the top trace is the velocity time history, and the bottom trace is the Husid plot, showing measurements of duration based on the 5% - 90% interval of the cumulative energy.
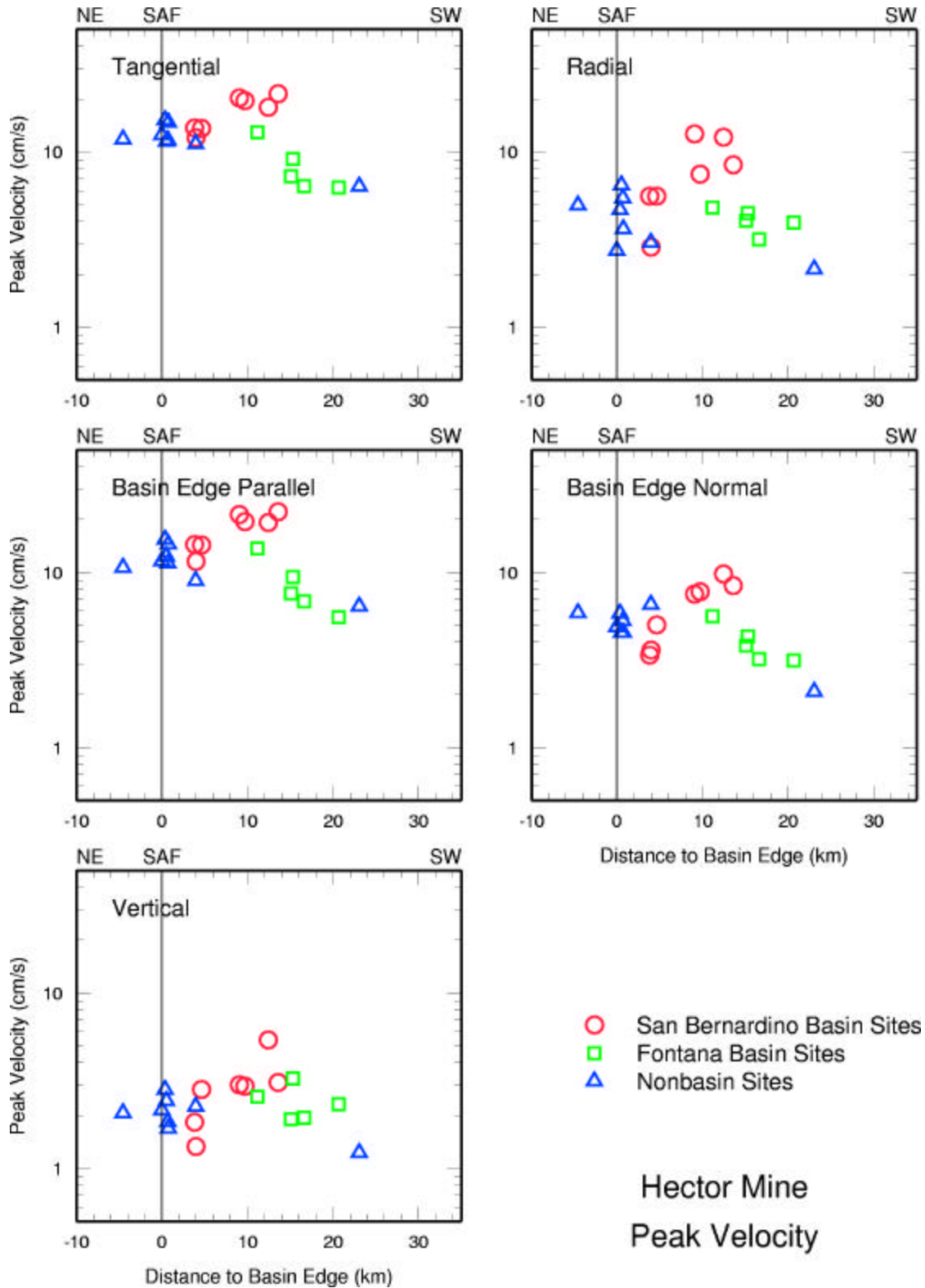
Figure 8. Distribution of peak velocity across profile A-A' in Figures 3 and 4 as a function of distance from the basin edge, marked by the San Andreas fault, shown by the vertical line, with positive values inside the basin, for five ground motion components.
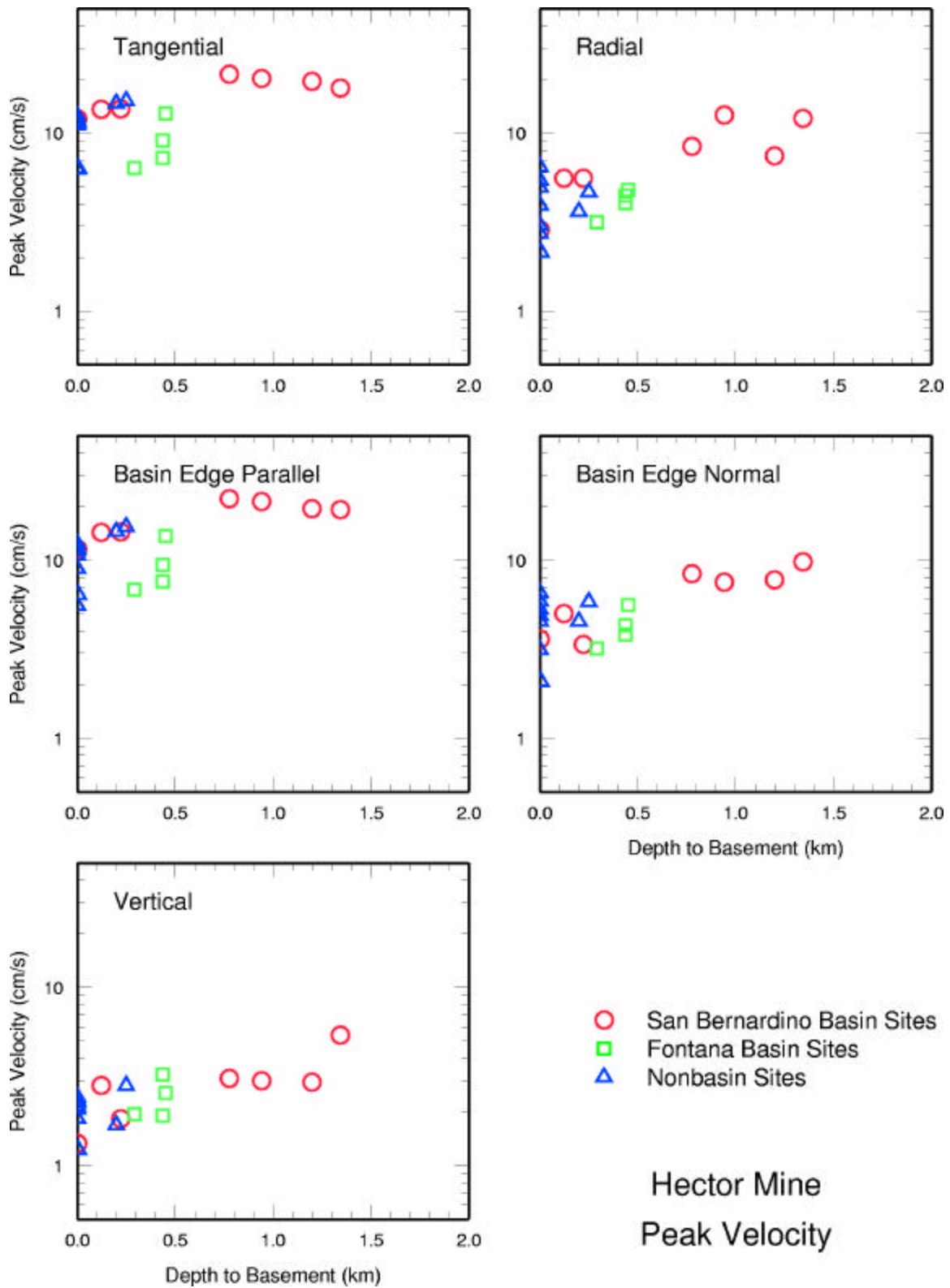
Figure 9. Distribution of peak velocity as a function of depth to basement for five ground motion components.
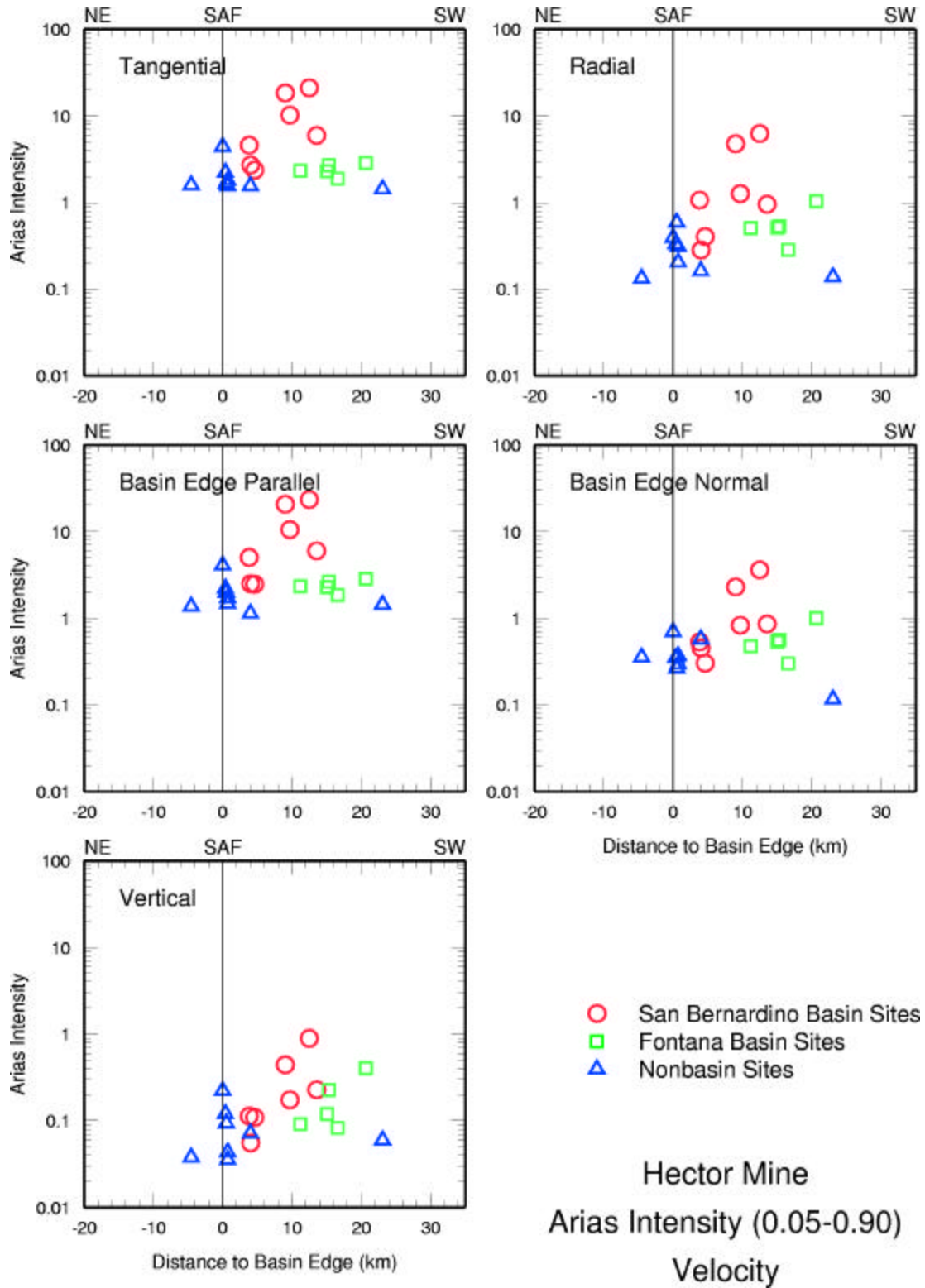
Figure 10. Distribution of Arias Intensity across profile A-A' in Figures 3 and 4 as a function of distance from the basin edge, marked by the San Andreas fault, shown by the vertical line, with positive values inside the basin, for five ground motion components.
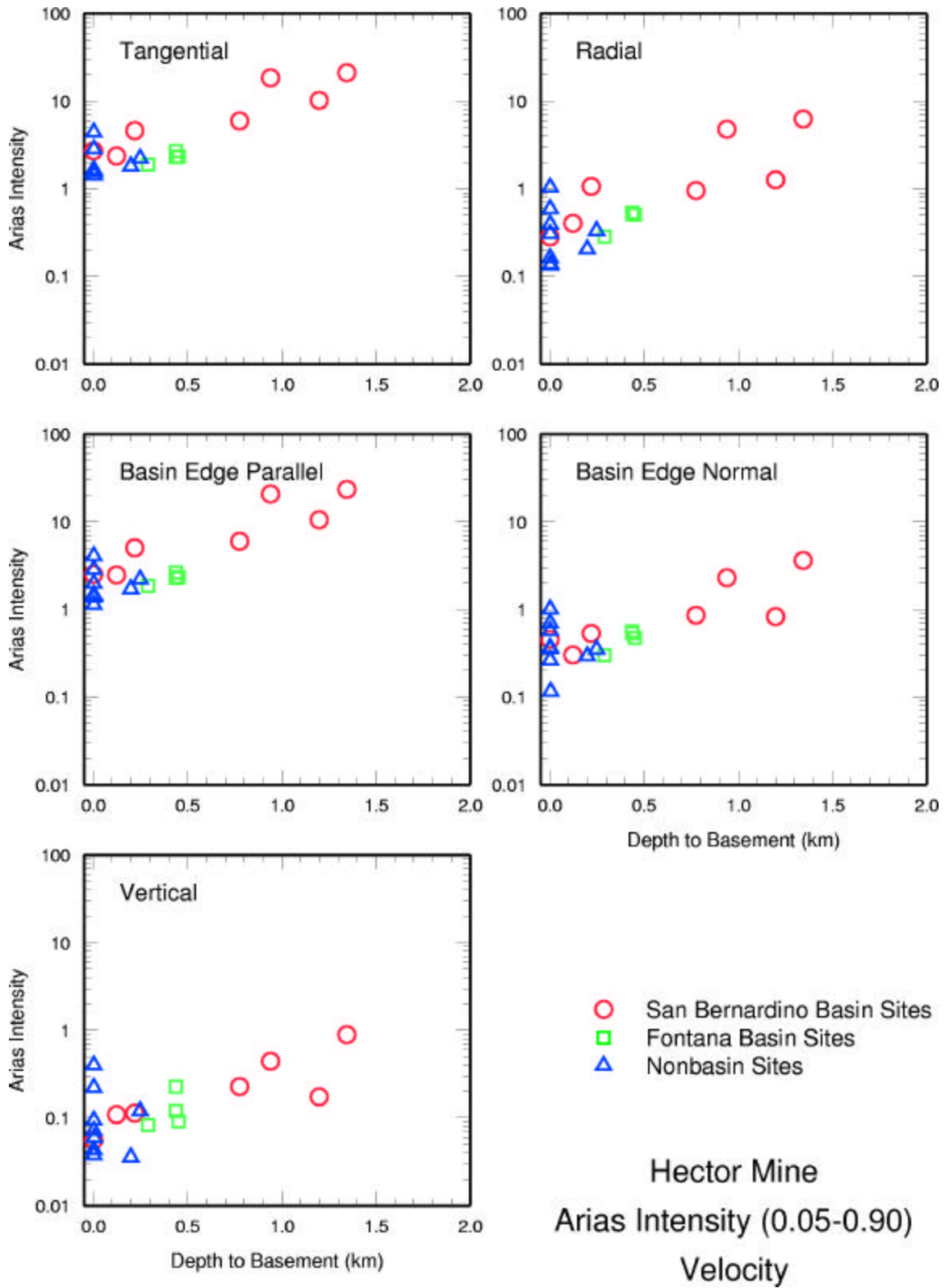
Figure 11. Distribution of Arias Intensity as a function of depth to basement for five ground motion components.
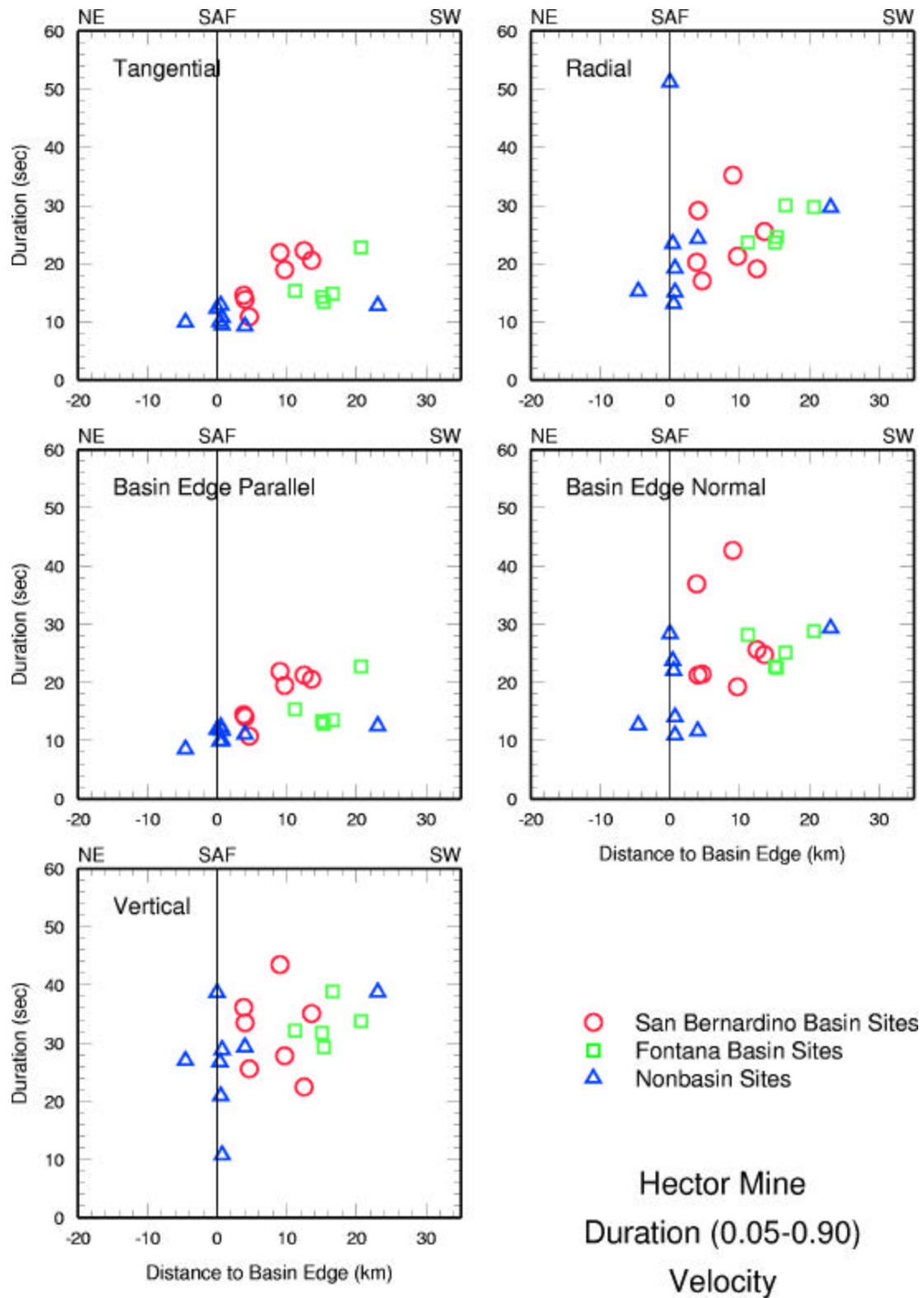
Figure 12. Distribution of Arias Intensity across profile A-A' in Figures 3 and 4 as a function of distance from the basin edge, marked by the San Andreas fault, shown by the vertical line, with positive values inside the basin, for five ground motion components.
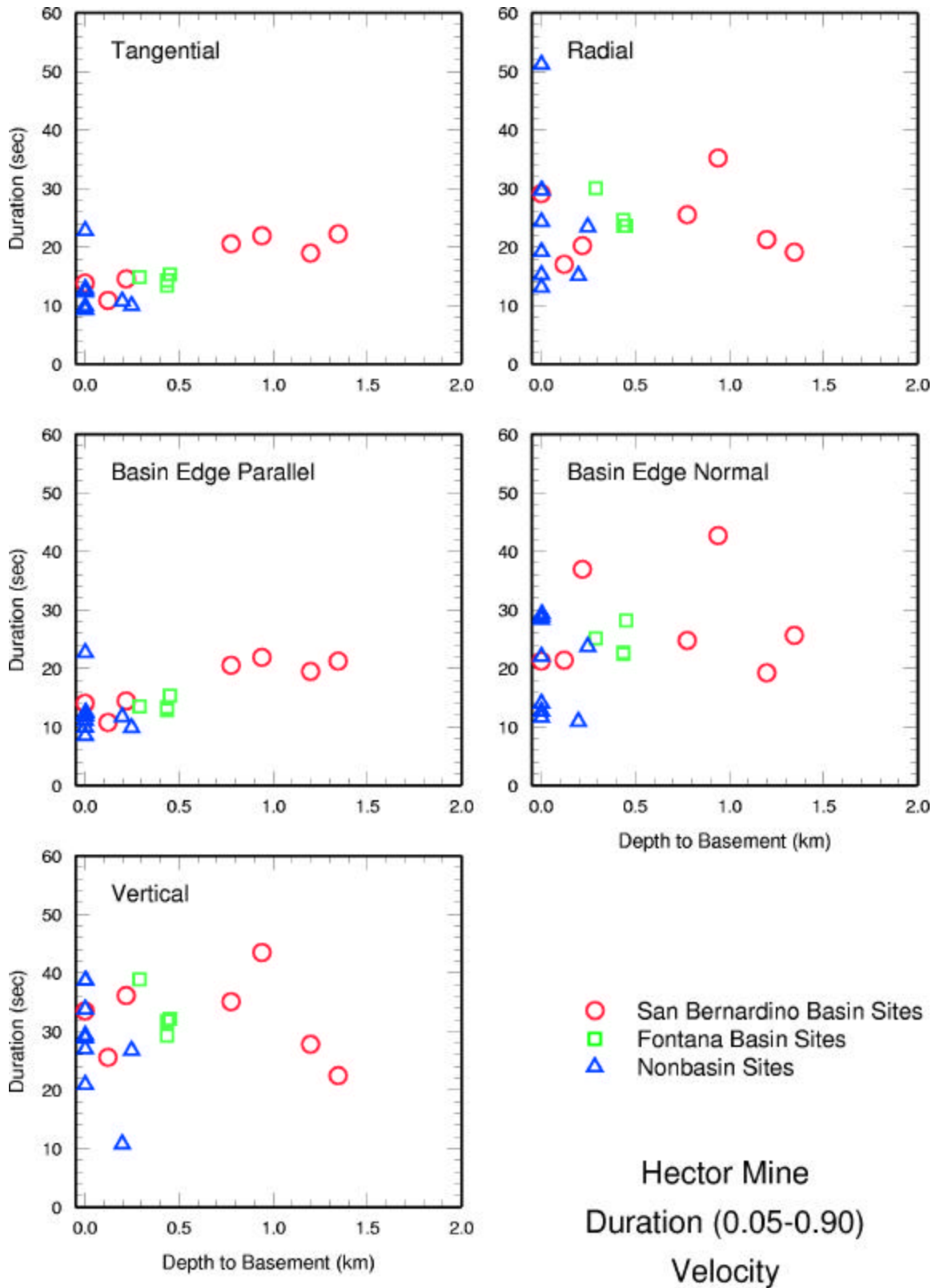
Figure 13. Distribution of Arias Intensity as a function of depth to basement for five ground motion components.